THEORETICAL TEMPERATURE FIELDS FOR THE STRIPA HEATER PROJECT

VOL. 1

Tin Chan, Neville G.W. Cook, and Chin-Fu Tsang

Lawrence Berkeley Laboratory
University of California
Berkeley, California 94720

This report was prepared by Lawrence Berkeley Laboratory under the University of California contract W-7405-ENG-48 with the Department of Energy. The contract is administered by the Office of Nuclear Waste Isolation at Battelle Memorial Institute.

September 1978

PREFACE

This report is one of a series documenting the results of the Swedish-American cooperative research program in which the cooperating scientists explore the geological, geophysical, hydrological, geochemical, and structural effects anticipated from the use of a large crystalline rock mass as a geologic repository for nuclear waste. This program has been sponsored by the Swedish Nuclear Power Utilities through the Swedish Nuclear Fuel Supply Company (SKBF), and the U. S. Department of Energy (DOE) through the Lawrence Berkeley Laboratory (LBL).

The principal investigators are L. B. Nilsson and O. Degerman for SKBF, and N. G. W. Cook, P. A. Witherspoon, and J. E. Gale for LBL. Other participants will appear as authors of the individual reports.

Previously published technical reports are listed below.

1. *Swedish-American Cooperative Program on Radioactive Waste Storage in Mined Caverns* by P. A. Witherspoon and O. Degerman. (LBL-7049, SAC-01).

2. *Large Scale Permeability Test of the Granite in the Stripa Mine and Thermal Conductivity Test* by Lars Lundstrom and Haken Stille. (LBL-7052, SAC-02).

3. *The Mechanical Properties of the Stripa Granite* by Graham Swan. (LBL-7074, SAC-03).

4. *Stress Measurements in the Stripa Granite* by Hans Carlsson. (LBL-7078, SAC-04).

5. *Borehole Drilling and Related Activities at the Stripa Mine* by P. J. Kurfurst, T. Hugo-Persson, and G. Rudolph. (LBL-7080, SAC-05).

6. *A Pilot Heater Test in the Stripa Granite* by Hans Carlsson. (LBL-7086, SAC-06).

7. *An Analysis of Measured Values for the State of Stress in the Earth's Crust* by Dennis B. Jamison and Neville G. W. Cook. (LBL-7071, SAC-07).

8. *Mining Methods used in the Underground Tunnels and Test Rooms at Stripa* by B. Andersson and P. A. Halen. (LBL-7081, SAC-08).

TABLE OF CONTENTS

VOL. 1

VOL. 2

ABSTRACT

The report concerns thermal conduction calculations for the three in-situ heater experiments at Stripa which constitute part of the Swedish-American Cooperative Program on Radioactive Waste Storage in Mined Caverns. A semi-analytic solution based on the Green's function method has been developed for an array of arbitrary time-dependent finite line heaters in a semi-infinite medium. This method as well as a three dimensional numerical model using IFD (Integrated Finite Difference) technique has been applied to model the field situations at Stripa. Comparison has demonstrated that the finite line source solution for the rock temperature is in excellent agreement with the numerical model solution as well as with a closed form finite cylinder source solution. It was found that maximum temperature rise in the rock within the two year experiment period will be 178°C for the 3.6 kW full-scale heater experiment, 345°C for the full-scale experiment with a 5 kW central heater and eight 0.72 kW peripheral heaters, and less than 200°C for the time-scaled experiment. The ring of eight peripheral heaters in the second full-scale experiment will provide a nominally uniform temperature rise within its perimeter a few weeks after turn-on. The high temperature zone is localized throughout the duration of all three experiments. Nevertheless, the effect of different spacings on the thermal interaction between adjacent radioactive waste canisters will be demonstrated by the time-scaled experiment. Detailed results are presented in the form of tables, temperature profiles and contour plots. Predicted temperatures have been stored in an on-site computer for real-time comparison with field data.

LIST OF TABLES

LIST OF FIGURES INTEGRATED IN TEXT

1. BACKGROUND

A potential solution to the problem of isolating radioactive wastes may lie in burying them in repositories excavated deep below the surface of the earth in hard rock. Several important questions must be answered before the effectiveness of such a solution can be assessed, or the design of a repository commenced. In addition to those questions which normally arise in connection with any major underground excavations, the disposal of radioactive wastes introduces a number of new isaues of which there is now virtually no experience. Important among these are the effects on a repository of the heat released by the radioactive decay of the wastes.

In the short term, this heat is apt to result in significant increases in the temperature of the rock around the canisters containing the wastes and of the waste canisters themselves. In the long term, the temperatures in a limited volume of rock around the whole repository will increase. The magnitude of these temperature changes will affect the entire strategy of the use and design of such a repository. The maximum temperatures that can be tolerated in the rock immediately around each canister will limit the size and heat output of each canister. These depend upon the nature of the radioactive waste (spent fuel or reprocessed waste, for example) and the period it may have to be cooled before burial. For any chosen specific heat output, the spatial distribution of canisters has a significant effect on the density with which the repository can be loaded.

2. PRELIMINARY CONSIDERATIONS

The significance of specific heat output and spatial distribution of canisters can be illustrated using classical solutions to the equations of heat conduction (Carslaw and Jaeger, 1959). For example, consider the temperature increases, ΔT, at periods of 2 years and 30 years after burial of heat sources approximating a point, a line, or a plane. The relevant solutions for sources of constant heat output are as follows:

i) Point source:

$$\Delta T = \frac{Q_{pt}}{4\pi kr} \operatorname{erfc} \frac{r}{(4\kappa t)^{\frac{1}{2}}} \tag{1}$$

where Q_{pt} = heat output of point (W);

r = radius (m);

k = thermal conductivity (W/m°C);

κ = thermal diffusivity (m^2/s); and

t = time (s).

ii) Infinite line source:

$$\Delta T = \frac{Q_{\ell}}{4\pi k} \left[\ell n \left(\frac{4\kappa t}{r^2} \right) - 0.58 \right] \tag{2}$$

(for large values of t), where Q_{ℓ} = heat output per unit length (W/m), and the remaining symbols are as defined above.

iii) Infinite plane source:

$$\Delta T = \frac{Q_{p\ell} (t)^{\frac{1}{2}}}{\kappa} \operatorname{ierfc} \frac{x}{(4\kappa t)^{\frac{1}{2}}} \tag{3}$$

where $Q_{p\ell}$ = heat output per unit area (W/m^2), x = distance from the plane (m), and the remaining symbols are as defined above.

For heat outputs of 1 kW for the point source, 0.1 kW/m for the line source, and 0.01 kW/m^2 for the plane source, the resulting temperatures at different distances from these sources have been calculated for periods of 2 years and 30 years after emplacement; these are plotted in Fig. 1.* For the purposes of these calculations, typical thermal properties for hard rock have been used, namely, a conductivity of 2.5 W/m°C, a density of 2600 kg/m^3, and

*Because of the vast amount of results obtained, only selected figures essential to the understanding of the report have been included in the text. For the convenience of those readers who wish to read off numerical values from the charts, a full set of figures is supplied in Vol. 2 of this report which may be obtained from National Technical Information Service, 5285 Port Royal Rd., Springfield, VA 22151.

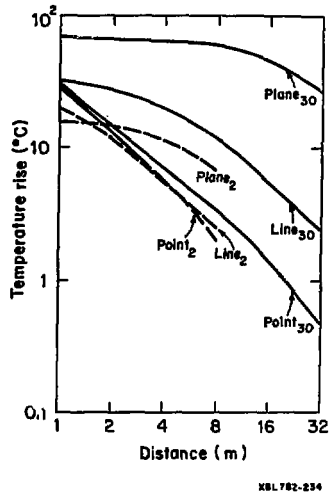

Fig. 1. Temperature rise at various distances from point, infinite line and plane heat sources. Subscript indicates time (years) after emplacement of the heat source. Thermal conductivity = 2.5 W/m°C, thermal diffusivity = 1.1×10^{-6} m^2/s.

a specific heat of 0.9 kJ/kg°C. These correspond to a thermal diffusivity of 1.1×10^{-6} m^2/s.

The most important characteristic to emerge from these results is the extent to which the temperatures vary around the three different kinds of sources. This variation is greater than a factor of 2, even though the heat output for each source has been chosen to correspond to a constant thermal loading of 0.01 kW/m^2, assuming that the point or line sources have a center-to-center spacing of 10 m. These variations in temperature are exaggerated in these simple calculations because the interaction of adjacent point and line sources has not been taken into account. However, the decrease in temperature with distance away from point and line sources is so great that the effects of interaction would not obscure the character of the source after a period of 2 years, not even after 30 years.

It is important to recognize the dominance of geometrical attenuation of the temperatures around these three different kinds of sources over distances of the order of 10 m and time periods of up to 30 years. The thermal effects on a potential repository cannot be defined adequately in terms of an average thermal loading (kW/m^2). An evaluation of these effects must take into account the geometrical disposition of the canisters within the repository and of the interaction between the temperature fields generated by these heat sources.

3. MOTIVATION FOR A COMBINED THEORETICAL AND EXPERIMENTAL STUDY

The above preliminary considerations are concerned mainly with the heat effects on the scale of the whole repository. But more drastic thermomechanical effects around each heat source are to be expected during the initial period when temperatures near the sources are estimated to rise quickly by 200-300°C or more, this amount decreasing with distance. The thermomechanical response of rock under such a temperature distribution has not been adequately studied.

Thus two types of problems arise in the heat effects of radioactive waste isolation in rocks:

1) the thermomechanical response of rock around each heat source,
2) the interaction among an array of heat sources.

In both cases, many critical issues have to be addressed. These range from in-situ rock property determination, heat conduction, presence of fractures, and occurrence of water flow in fractures to thermally induced displacements and stresses.

At the University of California Lawrence Berkeley Laboratory we have been developing various semi-analytical and numerical models to simulate heat conduction, thermal convection, fracture flow and thermomechanical problems. These are to be applied to model rock behavior when the rock is used as a radioactive waste repository. However, in reality, rock properties at the expected temperatures are not sufficiently well known; therefore the temperature fields around heat sources in rock may well differ significantly from those predicted. Also, the thermomechanical response of the rock to these temperatures is not well understood. To improve the adequacy of theoretical

models and to validate them, it is necessary to collect comprehensive data on temperatures and rock deformation and fracture in field experiments. Furthermore, these experiments will also identify the crucial physical phenomena that should be included in a numerical model. A tested and validated numerical model or procedure will be constructed, hopefully to describe expected rock behaviors for any given site considered for radioactive waste storage.

4. THREE EXPERIMENTS BEING MODELED

One of the more important practical limitations is that any reasonable experiments should not last more than two or three years. Furthermore, many national decisions concerning nuclear waste isolation will have to be made within the next two to five years. As can be seen from the results shown in Fig. 1, significant changes during the first few years in the temperatures around point or line sources of heat, which approximate individual waste canisters, are confined to within a short distance of each source. It follows that vital measurements of the temperature fields and rock behavior immediately around individual sources of heat, representing waste canisters, can be made within such a period of time, but that such measurements cannot be used to evaluate interaction between adjacent sources of heat.

Fortunately, the dimensionless factor governing heat conduction has the form $r/(4\kappa t)^{\frac{1}{2}}$, cf Eqs. (1), (2) and (3). Geometrically identical temperature fields can be generated around arrays of heat sources in shorter periods of time by appropriate reductions in linear scale. For example, if the linear scale of the heat sources is reduced to one-third, then the time scale must be accelerated by $(1/3)^{-2} = 9$ to maintain the same value of the dimensionless factor $r/(4\kappa t)^{\frac{1}{2}}$. Furthermore, by scaling the output of the heat sources appropriately, the actual values of the temperatures in these fields can be made identical. These properties make possible a time-scaled experiment in which the effects of interaction between adjacent heat sources over equivalently much longer periods of time than a few years can be measured in field experiments of moderately reduced linear scale.

Three separate experiments are underway at the Stripa mine in Sweden (Witherspoon and Degerman, 1978) (Fig. 2) to provide field data to develop and validate our understanding of the effects of heat sources on the behavior of a granitic rock. These comprise two experiments using full-scale electrical heaters to simulate the heat output of canisters of radioactive wastes of different ages and a time-scaled experiment to study the thermal interaction between waste canisters in a repository. These experiments form an integral part of LBL's contribution to the Swedish-American Cooperation Program on Radioactive Waste Storage in Mined Caverns.

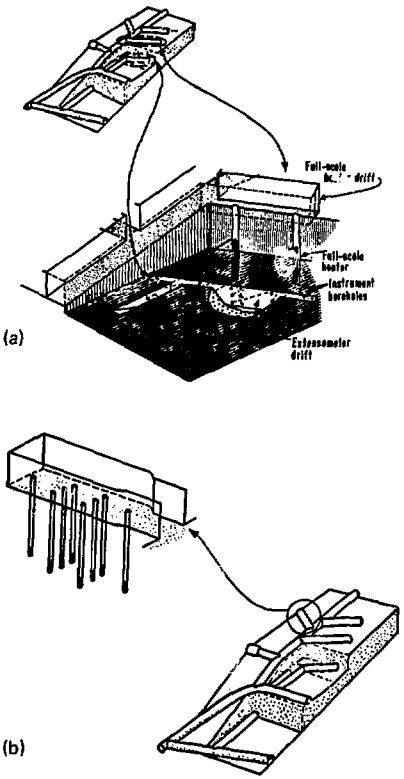

Fig. 2. Cut-away views of the LBL Full-scale (a) and time-scaled (b) heater experiments at Stripa (after Witherspoon and Degerman, 1978).

One of the full-scale experiments involves the burial of an electrical heat source about 0.3 m (1 ft) in diameter by 2.5 m (8 ft) in length into a vertical borehole 0.4 m (16 inches) in diameter drilled 5.5 m (18 feet) into the floor of a tunnel 338 m below surface. The second full-scale experiment is identical to the first, save that there are 8 peripheral heaters situated at a radius of 0.9 m (3 ft) around the main heat source (Fig. 3). The purpose of these peripheral heaters is to enable the ambient temperature of the rock around the main heat source to be raised at an appropriate stage of the experiment, in order t reproduce the higher ambient rock temperatures that are expected in the long term as a result of interaction between adjacent heaters. Finally, the time-scaled experiment (Fig. 4) has been designed using a linear scale of 0.32, which corresponds to a time scale of approximately 10.2, to provide a means of measuring the interaction between adjacent canisters over periods of time corresponding to decades rather than years. Practical considerations limit the number of time-scaled heat sources which can be emplaced,

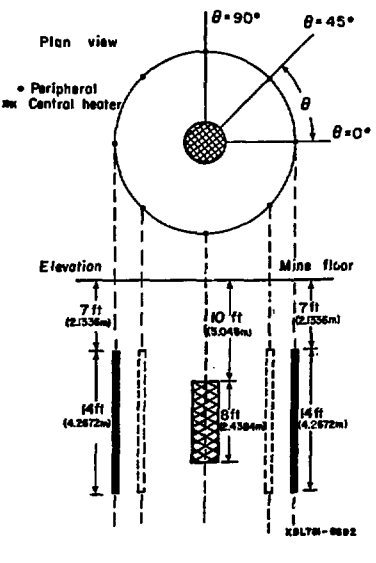

Fig. 3. Configuration of full-scale Experiment 2.

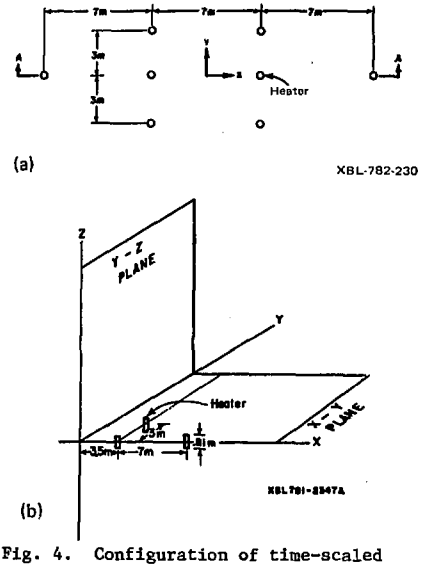

Fig. 4. Configuration of time-scaled heater experiment (Experiment 3) illustrating the coordinate system adopted.

but 8 heaters have been arrayed to provide measurements with a high degree of geometrical symmetry. Two spacings of heaters, namely 3 m and 7 m apart, correspond to spacings of about 9.6 m and 22.4 m on the full scale.

The first stage in the evaluation of these experiments has been to evaluate the temperature fields that may be expected in the rock around these heat sources at different times during the experiment on the basis of simple thermal conduction. In addition to being the first step toward the ultimate goal of developing viable theoretical models for radioactive repositories, these conduction calculations have (1) provided a rational basis for design of heaters, instrumentation and layout of the instruments, (2) been used as input for thermomechanical analysis, and (3) been stored in an on-site computer for instant graphic comparison with field data. Thus the work of the present authors involves not only the calculations but also writing the predicted data on magnetic tapes in a readily readable format and file structure. The file manipulation and graphics package implemented on the Modcomp computer at Stripa includes input programs specially tailored to read these predicted data tapes. Description of the data acquisition system, which includes the Modcomp computer, can be found in a report by McEvoy (1978).

Prior to the LBL heater experiments, a pilot heater experiment was carried out at the Stripa mine by Carlsson (1978) under the direction of Professor O. Stephansson, University of Luleå. This has provided valuable information for the planning of the LBL experiments.

5. SCOPE OF PRESENT WORK

The work reported here consists of thermal conduction modeling using semi-analytic and numerical methods. Section 6.1 contains the derivation of the solution for an array of finite-length line heaters in a semi-infinite medium, while Section 6.2 gives a brief review of the integrated finite-difference numerical technique. Results are presented in Section 7 for the various cases studied. These include a test case and two series of models for the in-situ heater experiments at Stripa. The test case was modeled using both semi-analytic and integrated finite-difference methods and served to verify the various computer programs by numerical comparison. The field cases were mostly modeled by the semi-analytical method. Series 1 of the field

cases, using average granite properties, was undertaken at a pre-design stage, whereas Series 2, using small specimen laboratory data for the thermal properties of Stripa granite, is intended for numerical comparison with field data. Results and implications are presented in Section 7.

6. THEORY

6.1 Semi-Analytic Solution

In order to render the heat transfer problem tractable by analytic methods for the field situations described above, we made the following assumptions:

1) conduction is the only mode of heat transfer,
2) the rock medium is homogeneous and isotropic,
3) the heaters and the rock medium have the same constant thermal properties,
4) the heaters are in direct thermal contact with the rock,
5) the rock medium can be considered infinite with uniform initial temperature or semi-infinite with the heater drift idealized as an isothermal or adiabatic boundary.

Under these assumptions the mathematical problem reduces to the solution of the heat diffusion equation:

$$\nabla^2 T - \frac{1}{\kappa}\frac{\partial T}{\partial t} = -\frac{Q}{k} \qquad (4)$$

where T = temperature

Q = heat generation per unit time per unit volume (in general a function of space and time)

t = time

k = thermal conductivity

$\kappa = k/\rho c$ = thermal diffusivity

ρ = density

c = specific heat capacity per unit mass.

This inhomogeneous partial differential equation is to be solved with appropriate initial and boundary conditions.

6.1.1 Green's Function Method

The Green's function method is a general technique to obtain closed form representations of the solutions to inhomogeneous linear partial differential equations with homogeneous or inhomogeneous boundary conditions. This method is well known among mathematical physicists and engineers and has been applied to a wide variety of physical problems (Morse and Feshbach, 1953; Carslaw and Jaeger, 1959; Chan and Ballentine, 1971). It can be shown (Morse and Feshbach, 1953) that the solution to the heat diffusion Eq. (4) is given by

$$T(\underline{r},t) = \frac{1}{k}\int_0^t\int_{V'} Q(\underline{r}',t')\; G(\underline{r},t;\,\underline{r}',t')dV'dt'$$

$$+\frac{1}{\kappa}\int_V T(\underline{r}',0)\; G(\underline{r},t;\,\underline{r}',0)dV'$$

$$+\int_0^t\int_S\left[\frac{\partial T(\underline{r}',t')}{\partial n'}\,G(\underline{r},t;\underline{r}',t') - \frac{\partial G(\underline{r},t;\underline{r}',t')}{\partial n'}\,T(\underline{r}',t')\right]dS'dt' \qquad (5)$$

where G is the Green's function, $\underline{r},t$ and $\underline{r}',t'$ are the spatial and time variables of the field and source points, respectively, V' denotes the volume occupied by the distributed source, and S encloses the domain V over which the solution is sought. The first term in Eq. (5) represents the temperature field due to a distributed volume source $Q(\underline{r}',t')$, the second term represents the effect(s) of the initial condition, and the third term the boundary conditions (prescribed temperature or normal temperature gradient). This last term, incidentally, forms the basis of the boundary integral equation method (Cruse and Rizzo, 1975). Formally, therefore, a solution in the form (5) can be found to the heat diffusion equation for an arbitrary heat source subject to any set of compatible initial and boundary conditions. The problem is to find the Green's function and to evaluate the integrals.

For the field situations studied in this report, under the assumptions stated above, it is necessary to evaluate only the first term in (5). The uniform initial temperature just corresponds to a shift in the temperature scale and an isothermal or adiabatic boundary condition can be simulated by images.

The Green's function in an infinite domain, or the temperature rise $G(\underline{r},t;\underline{r}'t')$ at position $\underline{r}$ at time t due to an impulse source of strength k at $\underline{r}'$ at time t' is (Morse and Feshbach, 1953)

$$G(\underline{r},t;\underline{r}',t') = \frac{K}{8[\pi\kappa(t-t')]^{3/2}} e^{\frac{-|\underline{r}-\underline{r}'|^2}{4\kappa(t-t')}} H(t,t') \tag{6}$$

where $H(t,t') = 0 , \quad t < t'$

$= 1 , \quad t > t'$

is the Heaviside step function.

6.1.2 Finite Line Source with Arbitrary Time-Dependent Power

For a line source of length 2b and arbitrary time-dependent heat generation rate $Q_\ell(t')$ per unit length per unit time, choosing a coordinate system such that $x' = y' = 0$, $-b \leq z' \leq b$ the temperature rise $\Delta T(x,t,z,t)$ is obtained by substituting Eq. (6) into the first term of (5) as

$$\Delta T(x,y,z,t) = \frac{K}{8k(\pi\kappa)^{3/2}} \int_0^t \frac{Q_\ell(t')}{(t-t')^{3/2}} \int_{-b}^{b} e^{-\frac{(z-z')^2}{4\kappa(t-t')}} e^{-\frac{(x^2+y^2)}{4\kappa(t-t')}} dz'dt' \tag{7}$$

Introducing variables $\mu = t-t'$ and $r = (x^2 + y^2)^{\frac{1}{2}}$ into Eq. (7),

$$\Delta T(r,z,t) = \frac{K}{8k(\pi\kappa)^{3/2}} \int_0^t \frac{Q_\ell(t-\mu)}{\mu^{3/2}} \int_{-b}^{b} e^{-\frac{(z-z')^2}{4\kappa\mu}} e^{-\frac{r^2}{4\kappa\mu}} dz'd\mu \tag{8}$$

From the definition of the error function and a simple change of variables, it is easily shown that

$$\int_{-b}^{b} e^{-\frac{(z-z')^2}{4\kappa\mu}} dz' = (\pi\kappa\mu)^{\frac{1}{2}} \left[\operatorname{erf}\left\{ \frac{z+b}{2(\kappa\mu)^{\frac{1}{2}}} \right\} - \operatorname{erf}\left\{ \frac{z-b}{2(\kappa\mu)^{\frac{1}{2}}} \right\} \right] \tag{9}$$

Substituting back into (8) yields

$$\Delta T(x,y,z,t) = \frac{1}{8\pi k}\int_0^t Q_\ell(t-\mu)\left[\operatorname{erf}\left\{\frac{z+b}{2(\kappa\mu)^{\frac{1}{2}}}\right\} - \operatorname{erf}\left\{\frac{z-b}{2(\kappa\mu)^{\frac{1}{2}}}\right\}\right]\frac{e^{-\frac{r^2}{4\kappa\mu}}}{\mu}\,d\mu \qquad (10)$$

In the special case of a constant power line source, the temperature rise can be expressed in an alternative form as follows. From (8) we have

$$\Delta T(x,y,z,t) = \frac{\kappa Q_\ell}{8k(\pi\kappa)^{3/2}}\int_{-b}^{b}\int_0^t \frac{e^{-\frac{s^2}{4\kappa(t-t')}}}{(t-t')^{3/2}}\,dt'dz'$$

$$= \frac{\kappa Q_\ell}{4k(\pi\kappa)^{3/2}}\int_{-b}^{b}\int_{t^{-\frac{1}{2}}}^{\infty} e^{-\frac{s^2\tau^2}{4\kappa}}\,d\tau dz' \qquad (11)$$

where $s^2 = x^2 + y^2 + (z-z')^2 = r^2 + (z-z')^2$ and $\tau = (t-t')^{-\frac{1}{2}}$. Now, from the definition of the complimentary error function, erfc, it follows that

$$\int_{t^{-\frac{1}{2}}}^{\infty} e^{-\frac{s^2\tau^2}{4\kappa}}\,d\tau = \frac{(\pi\kappa)^{\frac{1}{2}}}{s}\operatorname{erfc}\left(\frac{s}{\sqrt{4\kappa t}}\right) \qquad (12)$$

Inserting (12) into (11) we obtain

$$\Delta T(r,z,t) = \frac{Q_\ell}{4\pi\kappa}\int_{-b}^{b}\frac{\operatorname{erfc}\left[\left(\frac{r^2+(z-z')^2}{4\kappa t}\right)^{\frac{1}{2}}\right]}{[r^2+(z-z')^2]^{\frac{1}{2}}}\,dz' \qquad (13)$$

For points in the mid-plane (z=0) of the heater,

$$\Delta T(r,0,t) = \frac{Q_\ell}{2\pi k}\int_0^b \frac{\operatorname{erfc}\left[\left(\frac{r^2+z'^2}{4\kappa t}\right)^{\frac{1}{2}}\right]}{(r^2+z'^2)^{\frac{1}{2}}}\,dz' \qquad (14)$$

The special case, Eq. (14), was the expression used by Bäckblom (1978) to predict mid-plane temperatures for the pilot heater experiment at Stripa.

6.1.3 Finite Cylinder Source with Arbitrary Time-Dependent Power

Closed form integral solutions involving double integrals of Bessel function can be derived in a manner similar to that in the previous subsection for a constant, exponentially decaying (Mufti, 1971; Hodgkinson, 1977) or arbitrary time-dependent cylindrical heat source of finite height and finite radius (Chan and Remer, 1978).

6.1.4 Dimensionless Forms

In the present application where actual temperature measurements will be available for comparison, it is convenient to evaluate the dimensional expressions for temperature rises given above. For general usage it is often more convenient to reduce the expressions to dimensionless forms. Inserting dimensionless parameters

$$
\left.
\begin{aligned}
z^* &= \frac{z}{b} \\
r^* &= \frac{r}{b} \\
t^* &= \frac{Kt}{b^2} \quad , \quad \mu^* = \frac{K\mu}{b^2} \\
Q_\ell^*(t^*) &= \frac{Q_\ell(t)}{Q_{\ell o}} \quad , \text{ where } Q_{\ell o} = Q_\ell(0) \\
\Delta T^* &= \frac{\Delta T}{T_R} \quad , \text{ where } T_R = \frac{Q_{\ell o}}{8\pi k}
\end{aligned}
\right\} \tag{15}
$$

into (10) for the finite line source gives

$$
\Delta T^*(r^*,z^*,t^*) = \int_0^{t^*} Q^*_\ell(t^*-\mu^*) \left[\operatorname{erf}\left(\frac{z^*+1}{2\sqrt{\mu^*}}\right) - \operatorname{erf}\left(\frac{z^*-1}{2\sqrt{\mu^*}}\right) \right] \frac{e^{-\frac{r^{*2}}{4\mu^*}}}{\mu^*} \, d\mu^* \tag{16}
$$

which is entirely independent of material properties or heater length. Similarly, Eq. (13) reduces to

$$
\Delta T^*(r^*,z^*,t^*) = 2 \int_{-1}^{1} \frac{\operatorname{erfc}\left[\left| \frac{r^{*2} + (z^* - z')^2}{4t^*} \right|^{\frac{1}{2}} \right]}{\left[r^{*2} + (z^* - z')^2 \right]^{\frac{1}{2}}} \, dz' \tag{17}
$$

Equations (15) to (17) allow one to convert the temperatures for one particular set of heater power and thermal properties to those for another set. Thus, for example, the temperature rise is directly proportional to heater power per unit length and the quasi-steady state temperature rise is inversely proportional to the thermal conductivity.

6.1.5 An Array of Heaters in a Semi-Infinite Medium

Consider first an array of H parallel (finite line or finite cylinder) heaters in an infinite medium. Let $Q_h(t)$ be the heat generation rate per unit dimension (per unit length for line, per unit volume for cylinder); $2b_h$ be the length, and a_h be the radius (only for the finite cylinder case) for the h^{th} heater; t_h be the time at which it is switched on; and (x_h, y_h, z_h) be the Cartesian coordinates of the mid-point of its axis in a chosen coordinate system with the z-axis oriented parallel to the heaters. The temperature rise $\Delta T(x,y,z,t)$ at a point (x,y,z) in an infinite medium at time t is then given by

$$\Delta T_{total}(x,y,z,t) = \sum_{h=1}^{H} \Delta T_h(r_h, z-z_h, t-t_h | Q_h, b_h, a_h) \tag{18}$$

where $r_h = [(x-x_h)^2 + (y-y_h)^2]^{\frac{1}{2}}$ and $\Delta T_h(r,z,t-t_h|Q_h,b_h,a_h)$ designates the temperature rise caused by the h^{th} heater obtained by substituting the appropriate variables and parameters into ΔT of Eq. (10) or the corresponding cylindrical source solution, given in Chan and Remer (1978).

The effect of a plane adiabatic or isothermal boundary at $z = z_o$ can be simulated with positive or negative images, respectively. Thus the temperature rise caused by the array of heaters in a semi-infinite medium is

$$\Delta T_{total} = \sum_{h=1}^{H} \Delta T_h(r_h, z-z_h, t-t_h | Q_h, b_h, a_h) + \sum_{h=1}^{H} \Delta T_h(r_h, z-2z_o + z_h, t-t_h | \pm Q_h, b_h, a_h) \tag{19}$$

Here the positive or negative sign applies to an adiabatic or isothermal boundary, respectively.

On the basis of the theory presented above, two computer programs, FILINE and CYNDER, have been developed. FILINE calculates the temperature distribution in a semi-infinite medium arising from a three-dimensional array of finite-length line heaters with arbitrary time-dependent heat generation rate by evaluating Eqs. (10) and (19). CYNDER does a similar calculation for cylindrical heat sources of finite length and finite radius by evaluating the double integral solution given in Chan and Remer (1978) instead of Eq. (10). Initial results have been presented by one of the authors (T.C.) at the Stripa Project Review Meetings in Berkeley, August 1977 and January 1978.

Comparison of numerical results using FILINE and CYNDER (see Section 7) has demonstrated that the finite line model is sufficiently accurate for all practical purposes. Consequently, the majority of field situations have been modeled using FILINE which is computationally very efficient. As an illustration, the temperature field at 8000 points in three-dimensional space at 150 values of time, due to the eight-heater array in the time-scaled experiment, requires 3000 C.U. (LBL CDC-7600 computing unit) to compute, corresponding to 1/400 C.U. per space-time point.

Computational efficiency is an important issue since the predicted temperatures are to be stored in an on-site computer for contour plotting. Since the temperature field for two of the experiments is three-dimensional, each data file for contour and time-history plotting has to contain around 10^6 space-time points. Another distinct advantage of this semi-analytical method is that if the temperatures at a few specific points are required it is necessary only to do the calculations for these points. By contrast, in numerical methods, such as finite difference or finite element, the temperatures have to be calculated over the whole domain. Furthermore, it may be difficult to construct a numerical model to ensure an output value for every location of interest and, therefore, one must sometimes resort to interpolation which adversely affects the accuracy. Thus the amount of human as well as computational effort involved may differ by orders of magnitude. This point is especially important during the design stages when decisions on the geometrical configuration of the experiments and instrumentation have to be made on the basis of prompt response from the modeler.

6.2 Numerical Model "CCC"

The numerical model "CCC" (for Conduction-Convection-Consolidation) developed at the Lawrence Berkeley Laboratory (Lippmann et al., 1977) for geothermal modeling has been used for heat conduction calculations for some of field situations. This program solves coupled equations of heat and fluid transport by means of an integrated finite difference method with an efficient explicit-implicit iterative scheme for time integration (Edwards, 1972; Narasimhan and Witherspoon, 1976). Vertical consolidation or rebound is incorporated assuming the one dimensional consolidation theory of Terzaghi. The model is capable of handling one-, two-, or three-dimensional steady-state or transient, nonlinear (conductive and convective) heat and fluid flow in a heterogeneous isotropic, nonisothermal, saturated porous rock or soil medium. Thermal and hydraulic properties may be temperature and/or pressure dependent; deformation parameters may be nonlinear and nonelastic. The theoretical basis and numerical techniques are described in references quoted above.

In the present application only heat conduction problems are considered. When ground water is present, as appears to be the case for the Stripa site, it may be necessary to invoke the full capability of the "CCC" program. At present the CCC program cannot handle time-dependent heat sources or radiative heat transfer but only minor modifications are necessary to incorporate these.

7. RESULTS AND DISCUSSION

7.1 Test Case

To verify the program FILINE, based on the finite line source solution, a test case was analyzed. This test case consists of a 1 kW constant power cylindrical heat source approximately 2.5 m in length and 0.2 m in radius (corresponding to the dimensions of the full-size heater and heater hole respectively) implanted in granitic rock. Thermal properties, of Set 1 in Table 1, were assumed for both the heater material and the rock medium, unless otherwise stated. Temperature rise above ambient was calculated using the following three models:

Model T1: Constant power finite cylinder in infinite medium using program CYNDER based on Green's function solution

Model T2: Constant power finite line in infinite medium using program FILINE based on Green's function solution

Table 1. Material Properties of granite used in thermal calculations.

Property[a]	Unit	Set 1[b]	Set 2[c]
Density, ρ	kg/m	2600	2600
Specific heat, c	J/(kg°C)	897	837
Thermal conductivity, k	W/(m°C)	2.5	3.2
Thermal diffusivity, κ	m^2/sec	1.078×10^{-6}	1.47×10^{-6}

[a] Only thermal conductivity and thermal diffusivity are required for the calculations. The other two are also given since thermal diffusivity is usually deduced from measured values of conductivity, density, and specific heat.

[b] Average granite properties used in Model Series 1.

[c] Based on laboratory data for Stripa granite (Pratt et al., 1977) used in Model Series 2. Thermal conductivity decreases with temperature. The value of thermal conductivity used here corresponds to the laboratory data at approximately 100°C.

Model T3: Constant flux* finite cylinder model using the CCC program with boundary conditions as illustrated in Fig. 5.

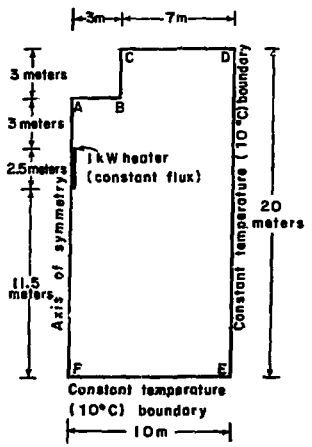

Fig. 5. System geometry and boundary conditions for CCC model of the test case. ABC - Newton's Law of Cooling with heat transfer coefficient 3.4 $W/m^2\,°C$; CEDF - isothermal or adiabatic boundary.

*A constant flux CCC model was used mainly to demonstrate that the details of the heater assembly (whether behaving as constant power or constant flux source) had little effect on the rock temperature. The two kinds of sources differ only by a transient of very short duration compared with the time of interest.

Comparison of temperature rises at the wall of the heater hole (where the difference is expected to be largest) as predicted by T1 and T2 (see Table 2) shows that except at very short times, there is excellent agreement, as one may expect from the short thermal diffusion time ($t_d \sim a^2/4\kappa \sim 0.2^2/4 \times 10^{-6}$ sec. $= 10^4$ sec. $\sim$ 0.1 day) across the radius of the heater and the small heat capacity of the heater assembly.

Table 2. Comparison of temperature rises at the wall of heater-hole ($r = 0.203$ m, $z = 0$) due to a 1 kW finite cylinder source[a] and a 1 kW finite line source.[b,c]

Time (day)	Temperature Rise (°C)		Difference	
	Cylinder	Line	°C	%
1	22.586	23.210	0.624	2.7
2	30.768	31.099	0.331	1.1
3	35.458	35.689	0.231	0.6
5	40.947	41.102	0.155	0.4
10	47.281	47.386	0.105	0.2
50	56.812	56.889	0.077	0.1
100	59.199	59.276	0.077	0.1
730	62.879	63.031	0.152	0.2

[a] Length = 2.44 m, radius = 0.203 m.

[b] Bäckblom (1978) has made a similar comparison.

[c] Material properties of Set 1 in Table 1 were used.

Various profiles of temperature rise from Model T2 have been plotted in Figs. 6-8. In these as well as in other figures, r,z and R,Z have been used interchangeably. Temperature rise, ΔT, rather than actual temperature, T, has been plotted because the former quantity is directly proportional to heater power. It is observed that there is a very steep radial temperature gradient within a radius of 0.5 m from the heater centerline throughout the 730 day period (Fig. 6). In general, temperature increases with time, while thermal

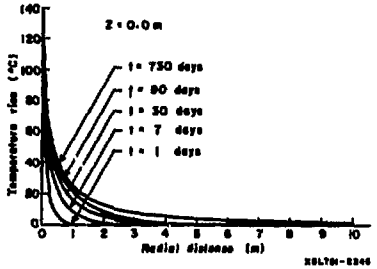

Fig. 6. Temperature rise in an infinite medium as a function of radial distance from 1 kW, 2.5 m-long line heater at different times. Thermal conductivity = 2.5 W/m°C, thermal diffusivity = 1.078×10^{-6} m^2/s.

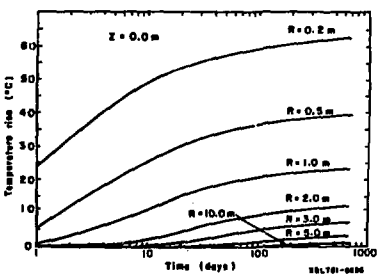

Fig. 7. Temperature rise in an infinite medium due to a 1 kW, 2.5 m-long line heater as a funtion of time at various radial distances. Thermal conductivity = 2.5 W/m °C, thermal diffusivity = 1.078×10^{-6} m^2/s.

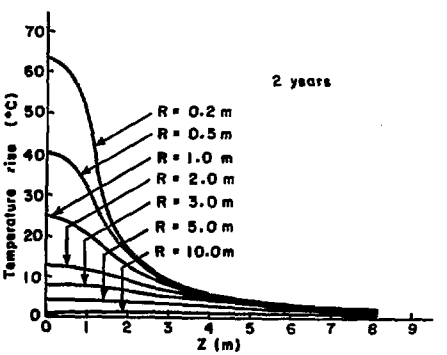

Fig. 8. Temperature rise in an infinite medium as a function of axial distance from the mid-plane of a 1 kW, 2.5 m-long line heater at various radial distances two years after emplacement. Thermal conductivity = 2.5 W/m °C, thermal diffusivity = 1.078×10^{-6} m^2/s.

gradients at the outer boundary of the heated zone decrease with time. There is little change in the temperature field between 90 and 730 days (Fig. 6). In fact, the temperature does not change by more than 2°C anywhere over the time interval 200-730 days (Fig. 7). Table 3 lists the time required for the temperature rise at various radial distances to reach 50%, 75%, and 90% of its value at the end of 730 days. Evidently, the temperature field within a radius of 2 m of the heater may be said to have attained a quasi-steady state in less than one year. Figure 8 illustrates the rapid drop of temperatures beyond the top of the heater for small radial distances.

Table 3. Time required for temperature rise (ΔT) at various radial distances (r) to reach 50%, 75% and 90% of the value at the end of 730 days--Test Case (1 kW full-scale heater).

r,m	ΔT (730 days)	Time, Days		
		50%	75%	90%
0.2	63.0	2.0	8.4	45.0
0.5	40.2	4.8	20.0	80.0
1.0	24.5	12.5	40.0	140.0
2.0	13.0	36.0	105.0	300.0

Results from Model T3 in which Newton's law of cooling with a heat transfer coefficient of 3·4 $W/m^2°C$ was assumed at the drift boundary ABC, Fig. 5, and isothermal boundary condition was applied at CDEF, Fig. 5, are presented in Figs. 9-11. A slightly different set of thermal properties ($k = 2.5 W/m°C$, $\kappa = 1.15 \times 10^{-6}$ m^2/sec) has been used. Consequently, the numerical values given in these figures are not exactly comparable to the other two models. Certain qualitative features, however, can be noted.

- The temperature field is asymmetric due to the convective boundary at the periphery of the drift (Figs. 9 and 11).

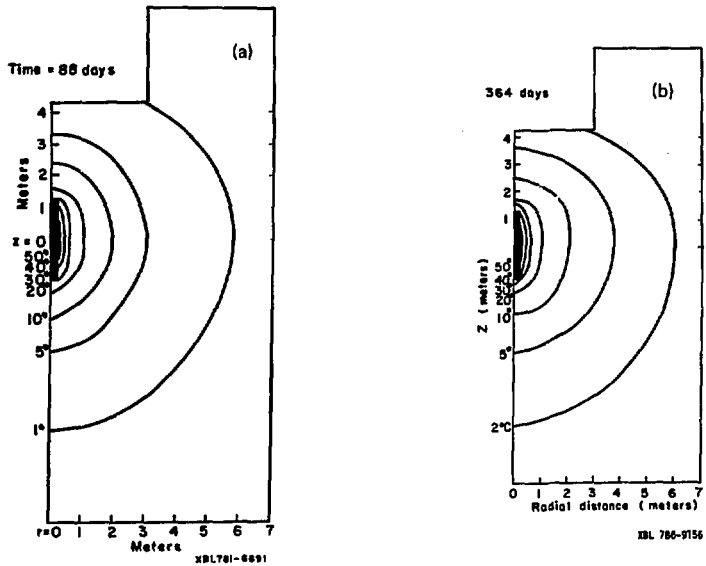

Fig. 9. Isotherms of temperature rise on day 88 and day 364 for the model depicted in Fig. 5 with CDEF as isothermal boundary; vertical section. Thermal conductivity = 2.5 W/m°C, thermal diffusivity = 1.15×10^{-6} m^2/s.

- There are only slight temperature increases in the rock around the drift implying that isothermal boundary condition would be a reasonable first approximation (Fig. 9).
- The heated zone is localized throughout the modeled period (Fig. 9, see also Fig. 6 and Fig. 13). This is due to the low thermal diffusivity of granite. Although granite has relatively high thermal diffusivity among crystalline rocks, it is still a poor thermal conductor compared with other materials. It can be seen from Fig. 6 (also Fig. 16 below) that the 50% and 25% (of the maximum ΔT in the rock) incremental isotherms migrate by less than 1 m and 2 m respectively in a radial direction from the heater in two years.

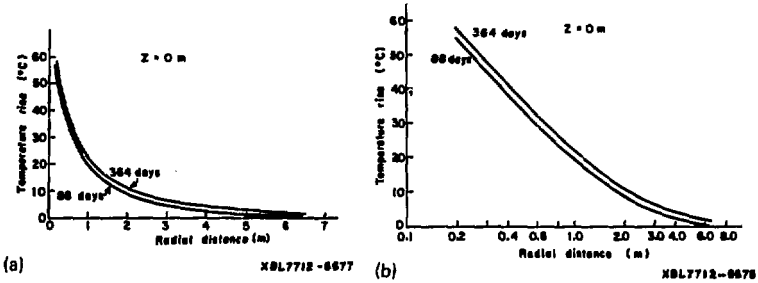

Fig. 10, a & b. Temperature rise as a function of radial distance along heater mid-plane for the same model as in Fig. 9, (a) linear scale, (b) semilog scale. Thermal conductivity = 2.5 W/m°C, thermal diffusivity = 1.15×10^{-6} m^2/s.

- o A steady-state is reached in 364 days as a result of the artifact of an isothermal boundary CDEF of Fig. 5, at a finite radial distance, acting as a spurious heat sink.*
- o The temperature rise along mid-plane exhibits a logarithmic r-dependence in the range $0.2 \leq r \leq 2$m in qualitative agreement with Eq. (2), Fig. 10b.

For the purpose of numerical comparison, two additional runs, with isothermal and adiabatic boundary conditions respectively at CDEF, were made, this time using thermal properties Set 1 of Table 1. The very close agreement between the predictions of Models T2 (constant power finite line source) and T3 (constant flux cylindrical source), as shown in Fig. 12, confirms the consistency between the programs FILINE and CCC, which are based upon entirely different algorithms.

The agreement between the two models can be understood by examination of

*This spurious effect could have been avoided by moving the boundary CDEF to a sufficient distance from the heater. However, this line of approach has not been pursued further in the present work.

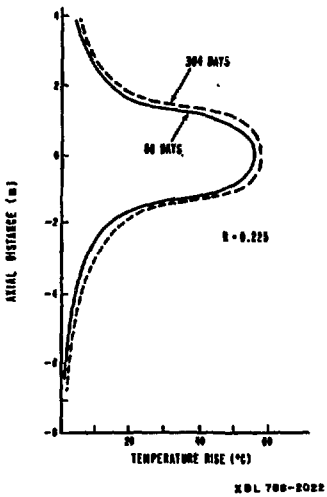

Fig. 11. Axial profile of temperature rise near heater for the same model as Fig. 9. Thermal conductivity = 2.5 W/m°C, thermal diffusivity = 1.15×10^{-6} m^2/s.

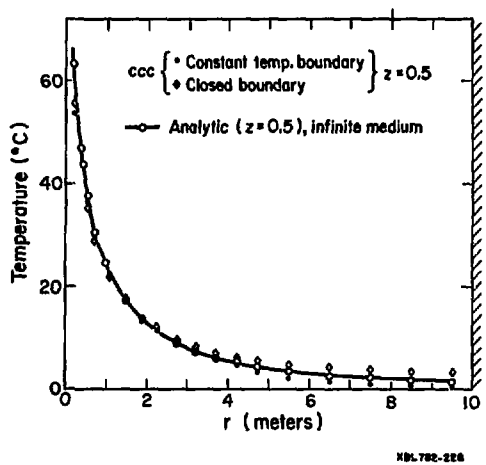

Fig. 12. Comparison of mid-plane radial profiles of temperature rise on day 364 as predicted by different models. Thermal conductivity = 2.5 W/m°C, thermal diffusivity = 1.078×10^{-6} m^2/s.

Fig. 7 for the constant power source. Except for the first few days the thermal gradient over r = 0.2 to 0.5 m remains practically constant. Physically what happens is that because of the small heat capacity of the heater assembly (or the cylinder of rock that replaces the heater in the models), the thermal gradient right next to the heater rises rapidly with consequent increase in the heat flux into the rock, so that a balance between the heat generated by the heater and the amount dissipated as flux across the heater surface is almost immediately achieved. From this one may hypothesize that the details of the heater assembly have little effect on the rock temperature. Furthermore, if the annulus of rock between r = 0.2 and 0.5 m decrepitates, there would only be minor perturbations in the form of a short transient on the temperature field in the rock outside unless the decrepitated rock acts as a nearly perfect thermal insulator. A similar conclusion cannot be reached regarding the temperatures of the heater, and detailed numerical analyses are necessary.

7.2 Field Cases

The three field cases in the Stripa mine described in Section 4 were modeled. Two series of thermal calculations were undertaken, the first with average granite properties (before laboratory data became available) providing preliminary predicted temperatures for experimental design, and the second with Stripa granite properties as measured in the laboratory (Pratt et al, 1977), yielding predicted temperatures that have now been stored in the on-site computer at Stripa for real-time comparison with field data. The two series of models are described separately below.

7.2.1 Model Series 1

In this series of models the peripheral heaters in one of the full-scale experiments were assumed turned on concurrently with the main heater, and material properties, Set 1 in Table 1, were used. When the thermal properties of Stripa granite were measured in the laboratory (Pratt et al, 1977), the thermal conductivity and diffusivity (Set 2 in Table 1) were found to have higher values than in Set 1. Consequently Model Series 1 overestimates the expected temperatures. It is a simple matter to scale the predicted temperature rises to those pertinent to Stripa granite using the scaling factors given in Section 6.1.4.

Table 4 summarizes the three field situations at Stripa, the source functions, boundary conditions, and computer programs used, and serves as an index for the figures pertinent to the various cases studied. The boundary conditions "isothermal" or "adiabatic" refer to the semi-infinite medium models where the floor of the heater drift is idealized as an isothermal or adiabatic plane boundary, respectively. The results are presented in Figs. 13-48 from which the following points emerge.

- The wall of the heater hole is very nearly isothermal and the isotherms are nearly vertical for small radial distances from the heater (see Figs. 13-15). However, even shortly after turn-on, a vertical thermal gradient exists, meaning that results predicted by an infinite line source model would not be accurate.
- The rock within a 2 m radius of the heater reaches a quasi-steady state in approximately one year (see Figs. 13-15), so that a two-year operation period is certainly sufficient.
- The heated zone remains localized throughout the two year-period (Figs. 13-15).
- The influence of the boundary condition at the drift floor is felt between one and three months after turn-on (Figs. 14 and 15).
- Adiabatic boundary condition leads to highest temperatures while isothermal boundary condition leads to highest vertical thermal gradients, as expected (Figs. 14 and 15). Comparison among Figs. 9, 13 and 14 reveals that the true convective boundary condition lies somewhere between the isothermal and infinite medium idealizations.
- The 25% incremental isotherm migrates by less than 1 m vertically and less than 2 m radially in two years (Fig. 16), with progressively slower spreading velocity since the volume of the shell of rock that has to be heated up is proportional to the thickness squared.
- Temperatures predicted using the three different boundary conditions are drastically different near the drift floor and quite similar near the mid-plane (Figs. 17 and 18). Relative difference between ΔT for the three cases are not negligible even along mid-plane for $r > 1m$ toward the end of the experiment (Fig. 19).

Table 4. Different cases in Stripa Thermal Model Series 1.

Field Situation	Model Designation	Source Function	Boundary Condition(s)	Program Used	Figures
Experiment 1: One 3.6 kW full-scale heater	1A	constant power	infinite medium	FILINE[a]	13,17,18,19
	1B		isothermal		14,16,17,18,19
	1C		adiabatic		15,17,18,19
Experiment 2: One 5 kW full-scale central heater and eight 1 kW peripheral heaters	2A	constant power, all heaters on	infinite medium		20,21,22,23,29,30,31
	2B		isothermal		24,25,26,29,31,31
	2C		adiabatic		27,28,29,30,31
	2D	constant power, only peripheral heaters on	infinite medium	FILINE	32,33,34,35
	2E		isothermal		36,37
	2F		adiabatic		38,39
Experiment 3: Eight time-scaled heaters (1.125 kW initial power)	3A	constant power	infinite medium	FILINE	40-44
	3B	constant power	isothermal	CCC[b]	45-48
	3C	constant power	adiabatic	CCC	45-48
	3D	one constant power time-scaled heater	adiabatic, cased borehole	CCC	

[a] FILINE = program based on closed form integral solution for finite line source (see Section 6.1).

[b] CCC = numerical code using integrated finite difference method.

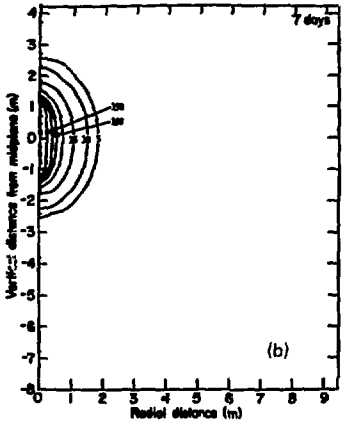

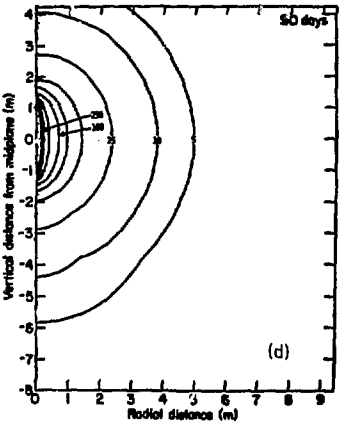

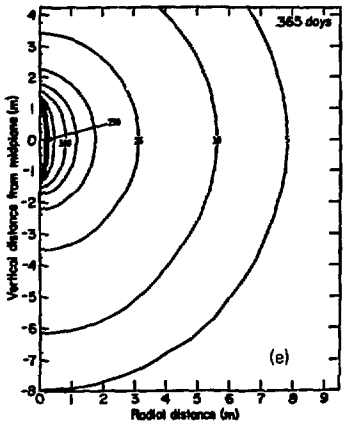

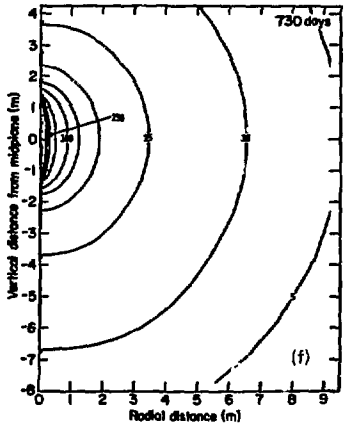

Fig. 13b, d, e, f. Isotherms of temperature rise (°C) in granite caused by one 3.6 kW full-scale heater at time = 7, 90, 365 and 730 days; vertical section, infinite medium model (1A). Thermal conductivity = 2.5 W/m°C, thermal diffusivity = 1.078×10^{-6} m2/s.

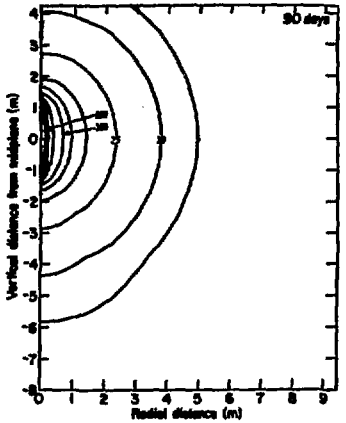

(13d)

XBL 785-8550

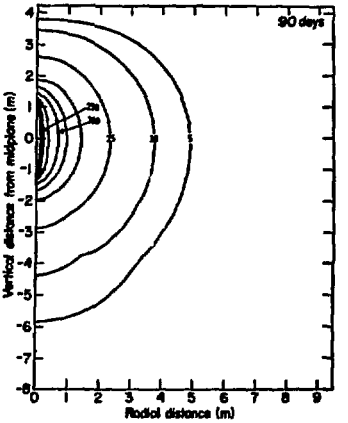

(14d)

XBL 785-8538

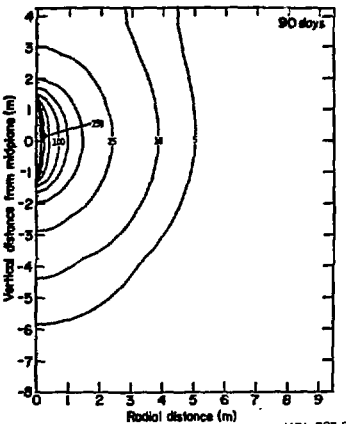

(15d)

XBL 785-8544

Figs. 13d, 14d, 15d. Isotherms of temperature rise (°C) in granite caused by a 3.6 kW full-scale heater at time = 90 days under three different assumed boundary conditions: infinite medium (Model 1A), Fig. 13d, heater drift modeled as isothermal boundary (Model 1B), Fig. 14d, and heater drift modeled as adiabatic boundary (Model 1C), Fig. 15d. Vertical section through axis of heater is illustrated. Thermal conductivity = 2.5 W/m°C, thermal diffusivity = 1.078×10^{-6} m^2/s.

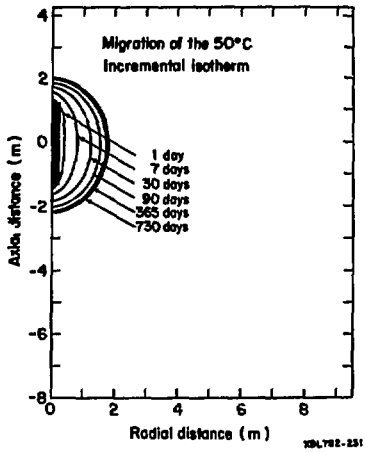

Fig. 16. Migration of the 50°C incremental isotherm as predicted by Model 1B. Thermal conductivity = 2.5 W/m°C, thermal diffusivity = 1.078×10^{-6} m^2/s.

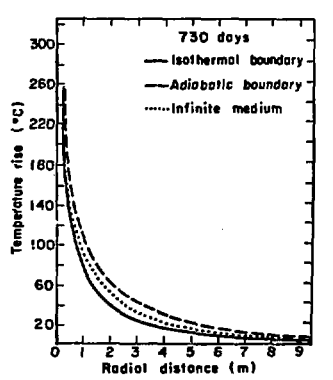

Fig. 19. Comparison of radial profiles of temperatures rise along heater mid-plane as predicted by Models 1A, 1B and 1C. Thermal conductivity = 2.5 W/m°C, thermal diffusivity = 1.078×10^{-6} m^2/s.

- Interaction between central and peripheral heaters (Experiment 2) is almost immediate with the 5°C and 100°C isotherms enveloping all the heaters in one and seven days, respectively (Figs. 20-22 and 24-27).
- The three-dimensional nature of the model is evident from the various vertical and horizontal sections (Figs. 20-22 and 24-28).
- A few weeks after turn-on, the ring of peripheral heaters produces a nominally uniform temperature rise within its perimeter (Figs 32-39, Models 2D, 2E and 2F). Thus these peripheral heaters physically duplicate a condition that might prevail in an actual repository where, over a period of several decades, heat from the interaction of large arrays of waste canisters raises the ambient rock temperature around a canister without introducing an additional thermal gradient.
- The ambient temperature caused by the peripherals is well in excess of 100°C (Fig. 35), even after scaling for thermal properties. A uniform temperature increase of 100°C induces approximately a milli-strain ($\varepsilon \sim \alpha\Delta T \sim 100 \times 10^{-5} = 10^{-3}$) which is already very significant for crystalline rock. Accordingly, it was decided that the power of peripheral heaters be reduced to give an ambient temperature rise of about 100°C. Furthermore, concurrent turn-on of all heaters which produces a condition resembling sequential emplacement of canisters in the repository (the ambient rock is hot shortly after emplacement), leads to very high temperatures (235°C after scaling for Stripa granite properties), exceeding the ratings of the extensometers and stressmeters within a 1 m radius of the main heater. To ensure that sufficient amounts of data are collected before instrument failure, it was decided that the peripheral heaters should be delayed. This latter schedule resembles the situation of simultaneous canister emplacement in a repository, i.e. ambient rock temperature is raised by the heat from other canisters in the array, only after quasi-steady state has been approached locally in the immediate vicinity of a particular canister.

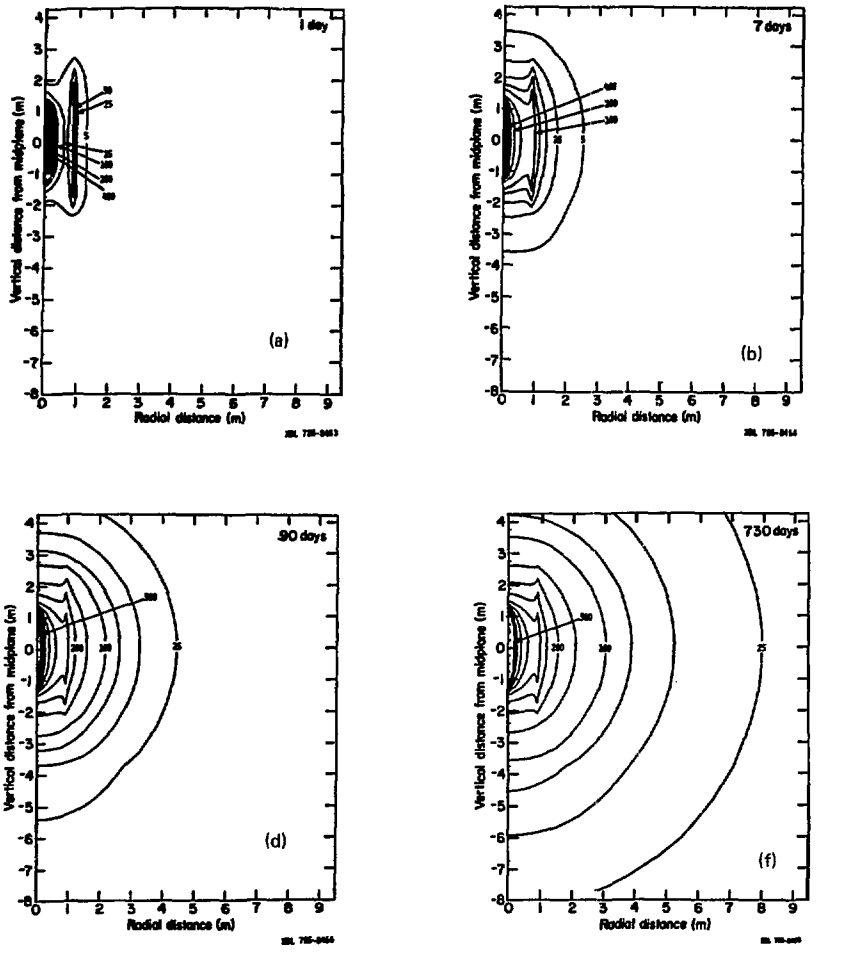

Fig. 20a, b, d, f. Isotherms of temperature rise (°C) in granite caused by a 5 kW full-scale central heater and a ring of eight 1 kW peripheral heaters (turned on simultaneously) at time = 1, 7, 90, and 730 days; vertical section through axes of central heater and one peripheral heater; infinite medium model (2A). Thermal conductivity = 2.5 W/m°C, thermal diffusivity = 1.078×10^{-6} m^2/s.

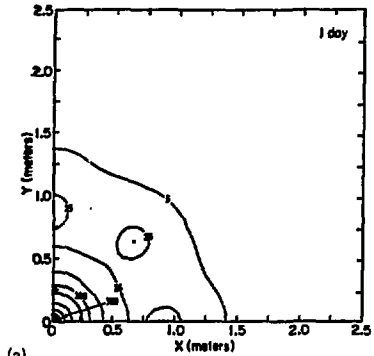

(a)

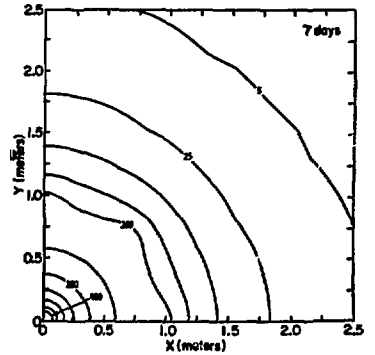

(b)

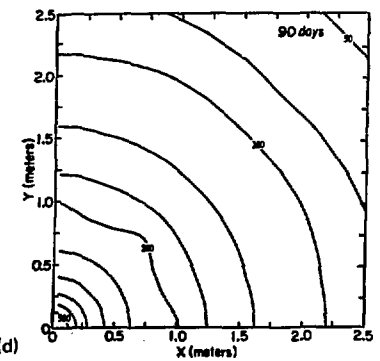

(d)

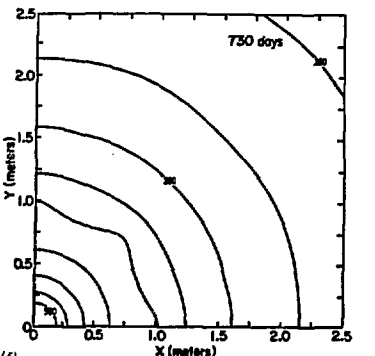

(f)

Fig. 22a, b, d, f. Isotherms of temperature rise (°C) in granite caused by a 5 kW full-scale central heater and a ring of eight 1 kW peripheral heaters (turned on simultaneously) at time = 1, 7, 90, and 730 days; horizontal section through mid-plane of heaters; infinite medium model (2A). Thermal conductivity = 2.5 W/m°C, thermal diffusivity = 1.078×10^{-6} m^2/s.

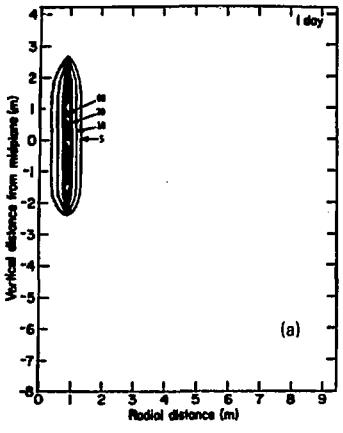

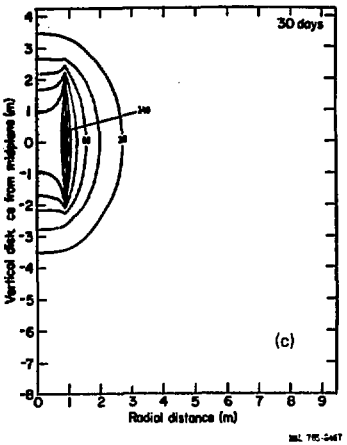

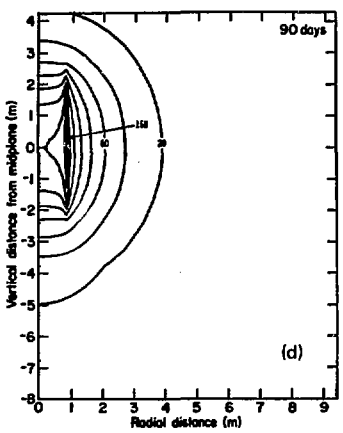

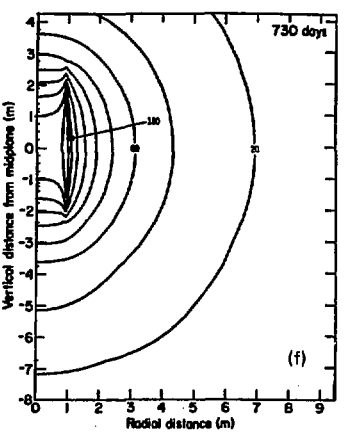

Fig. 32a, c, d, f. Isotherms of temperature rise (°C) in granite caused by a ring of eight 1 kW peripheral heaters at time = 1, 30, 90, and 730 days; vertical section through axis of one peripheral heater and the central axis of the ring; infinite medium model (2D). Thermal conductivity = 2.5 W/m°C, thermal diffusivity = 1.078×10^{-6} m^2/s.

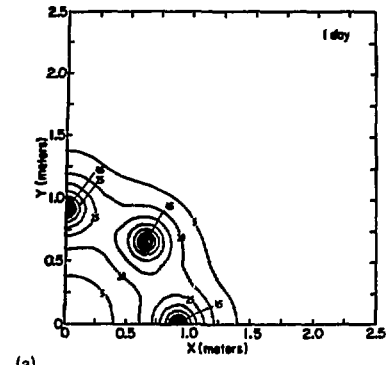

(a)

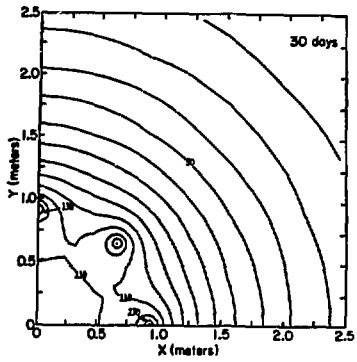

(c)

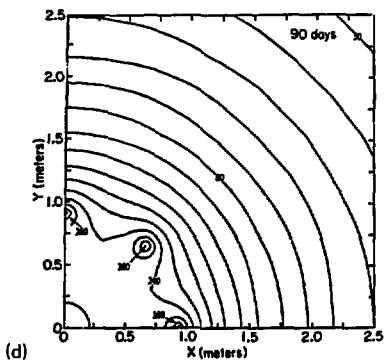

(d)

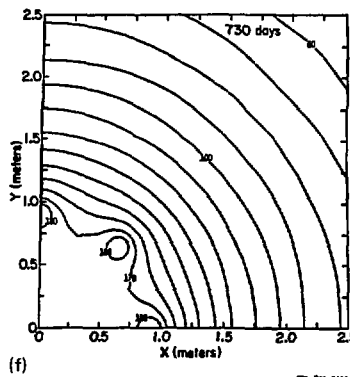

(f)

Fig. 34a, c, d, f. Isotherms of temperature rise (°C) in granite caused by a ring of eight 1 kW peripheral heaters at time = 1, 30, 90, and 730 days; horizontal section through mid-plane of heaters; infinite medium model (2D). Thermal conductivity = 2.5 W/m°C, thermal diffusivity = 1.078×10^{-6} m^2/s.

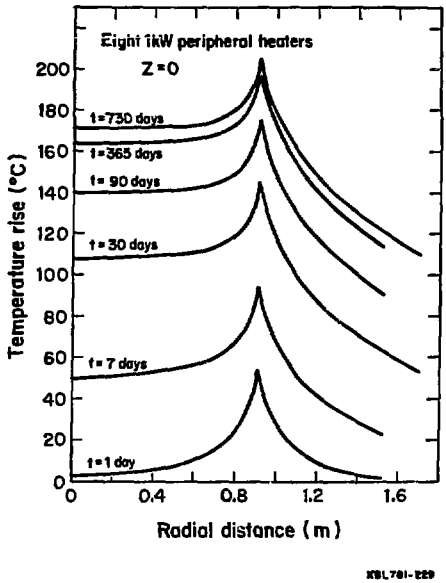

Fig. 35. Radial profile of temperature rise along mid-plane of ring of peripheral heaters at various times as predicted by Model 2D (infinite medium). Thermal conductivity = 2.5 W/m°C, thermal diffusivity = 1.078×10^{-6} m^2/s.

- Because of the proximity of the top of the peripheral heaters to the drift floor, their temperature field is influenced sooner and to a greater extent by the boundary condition (Figs. 36-39). This should be borne in mind when comparing field data with theory.

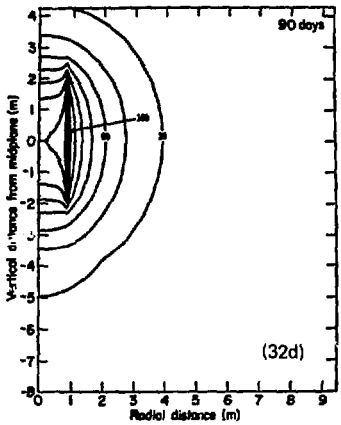

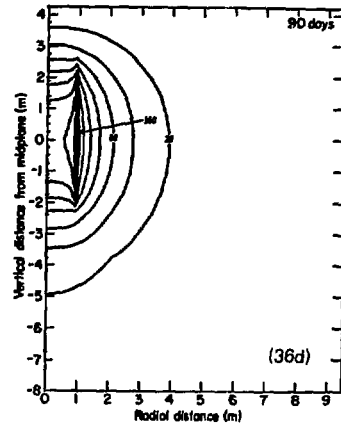

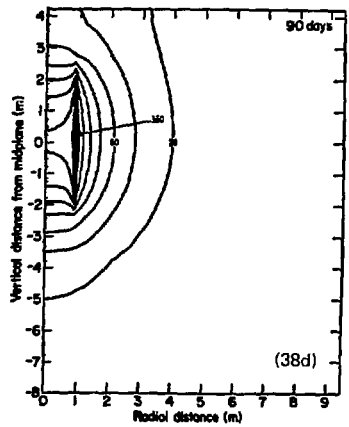

Fig. 32d, 36d, 38d. Isotherms of temperature rise (°C) in granite caused by a ring of eight 1 kW peripheral heaters at time = 90 days under three different assumed boundary conditions: infinite medium (Model 2D), Fig. 32d, heater drift modeled as isothermal boundary (Model 2E), Fig. 36d, and heater drift modeled as adiabatic boundary (Model 2F), Fig. 38d. Vertical section through axis of one peripheral heater and the central axis of the ring is illustrated. Thermal conductivity = 2.5 W/m°C, thermal diffusivity = 1.078×10^{-6} m^2/s.

- In the time-scaled experiments (Figs. 40-44) thermal interaction begins in about a week (in the form of merging of the 5°C incremental isotherm) between two heaters at 3 m spacing (corresponding to 9.6 m in full scale), and in about 3 months between two heaters at 7 m spacing (corresponding to 22.4 m in full scale). After two years (20.4 years full scale), all the heaters are interacting (at the 20°C or 30°C level), but the temperature distribution is still far from being uniform. Therefore, in designing a repository to ensure retrievability, it is important to carry out detailed canister arrangement studies rather than to use gross thermal loading as the sole

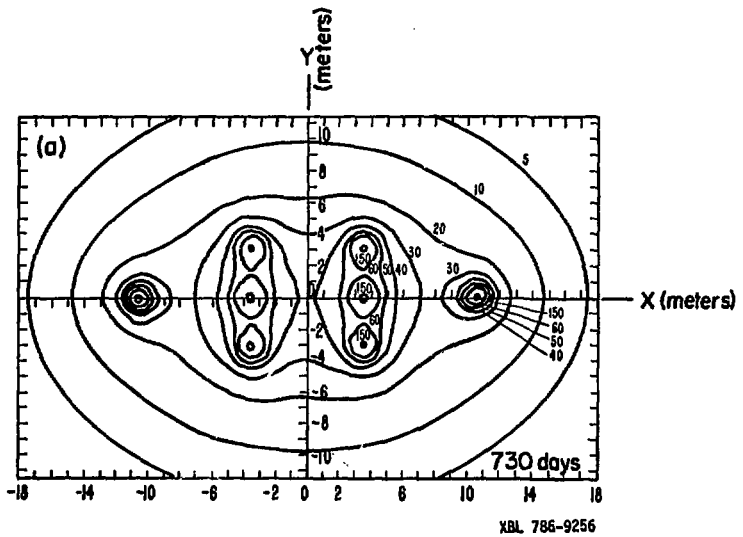

Fig. 40. Full-plane pattern of temperature rise in horizontal section through mid-plane of time-scaled experiment on day 730; constant source, Model 3A. Thermal conductivity = 2.5 W/m°C, thermal diffusivity = 1.078×10^{-6} m^2/s.

thermal criterion. The low isotherms have elliptical shape (ellipsoidal in 3-dimensional space) after two years, so that the time-scaled experiment does resemble a scaled down repository.

- o The scaling is correct. As an example, 30 days after turn-on the temperature rises by 30°C at 0.5 m from the heater at the end of the time-scaled array (Fig. 41). A similar temperature rise obtains at r = 1.6 m, one year after turn-on of the single 3.6 kW full scale heater (Fig. 14).
- o A coarse-mesh CCC model for the time-scaled experiment (Fig. 45) yields generally similar temperature fields (Figs. 46-48) to those predicted by the finite line model.
- o A CCC conduction calculation (case 3D) shows that only a negligible fraction of the time-scaled heater power will be lost through vertical conduction up the stainless steel heater canister. This result is reasonable in view of the very small cross-sectional area of the steel piping used as the canister.

7.2.2 Model Series 2

This series differs from the previous in two respects:

1) The peripheral heaters in Experiment 2 are assumed to be turned on 180 days after the central heater and operated at a power of 0.72 kW each.

2) Thermal properties, Set 2 in Table 1, as measured in laboratory specimens of Stripa granite (Pratt et al, 1977) were used.

A value of 3.2 W/m°C for the thermal conductivity was arrived at in the following manner. First, the CCC model T3 (see Section 7.1) with 3.6 kW power was run using the measured temperature-dependent thermal conductivity (Pratt et al, 1977)

$$k(T) = 3.60 - 0.3745 \cdot 10^{-2} T \quad (W/m°C) \quad .$$

Next, a few more runs of the same model were made with different constant thermal conductivity. It was found that a constant k = 3.2 W/m°C gives the best general agreement with the temperature-dependent thermal conductivity model.

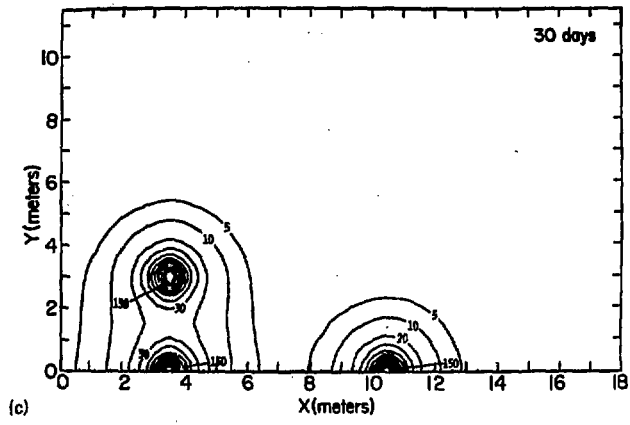

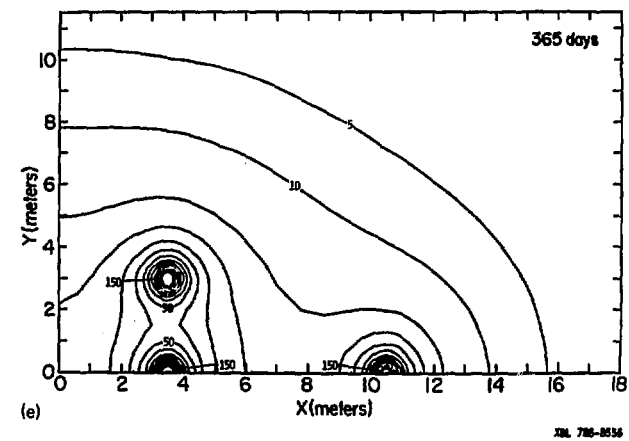

Fig. 41, c, e. Isotherms of temperature rise (°C) in granite caused by an array of eight constant 1.125 kW time-scaled heaters; horizontal section through mid-plane of the heaters; Model 3A. Only one quadrant is plotted because of the symmetry resulting from assumed istropy. Isotherms are at 10°C intervals unless otherwise indicated. Thermal conductivity = 2.5 W/m°C, thermal diffusivity = 1.078×10^{-6} m^2/s.

Five different cases using FILINE have been completed in this series, i.e., the infinite medium model for each of the three heater experiments and isothermal boundary model for the two full-scale experiments. Results are presented in Tables 5-7, in ΔT vs. time profiles (Fig. 49 for Experiment 1;* Fig. 50 for Experiment 2) and contours (Fig. 51 [infinite medium] and Fig. 52 [isothermal boundary] for Experiment 1; Fig. 53 [infinite medium] and Fig. 54 [isothermal boundary] for Experiment 2; and Figs. 55-59 for Experiment 3 [time-scaled experiment]). Constant power calculations for Experiment 3 giving conservative estimates are presented here. Results for decaying power will be available shortly.

The results do not reveal any qualitative difference from those of Series 1 except for the "two-step" nature of the radial profiles for Experiment 2 arising from the delayed turn-on of the peripheral heaters. Therefore, previous comments on Series 1 results that also apply here will not be repeated. Several important points can be noted:

- o Maximum temperature rises in the rock are 177.8°C in Experiment 1; 344.8°C in Experiment 2, and 199°C in Experiment 3.

Table 5. Time required for temperature rise (ΔT) at various radial distances (r) to reach 50%, 75% and 90% of the value at the end of 730 days--Stripa Thermal Model Series 2 (thermal properties, Set 2, Table 1), Experiment 1 (3.6 kW full scale heater).

r(m)	ΔT (730 days)	Time, Days 50%	75%	90%
0.203	177.8	1.5	7.4	37.5
0.5	114.0	4.2	16.7	71.0
1.0	70.3	11.3	37.0	131.0
2.0	37.2	29.3	90.0	243.0
5.0	12.6	118.0	258.0	458.0

*Experiment 1 = full scale 3.6 kW, Experiment 2 = full scale 5 kW with peripherals, Experiment 3 = timed-scaled experiment.

Table 6. Time required for temperature rise (ΔT) at various radial distances (r) to reach 50%, 75%, and 90% of the value at the end of 730 days--Stripa Thermal Model Series 2 (thermal properties, Set 2 of Table 1), Experiment 2 (5 kW full-scale heater with eight 0.72 kW peripheral heaters turned on 180 days later).

r (m)	ΔT (730 days)	Time, Days		
		50%	75%	90%
0.203	344.76	5.1	183.2	213.0
0.5	256.80	27.0	188.2	235.0
1.0	195.65	180.5	194.7	262.4
2.0	105.46	187.0	227.6	500.8
5.0	36.17	238.7	355.0	517.0

Table 7. Temperature rise (°C) at various radial distances and time for the Stripa full scale experiment 2 (5 kW full-scale heater with eight 0.72 kW peripheral heaters turned on 180 days later)-Model Series 2 (thermal properties, Set. 2, Table 1).

Time (day)	Radial Distance (m)					
	0.203	0.5	1	2	3	5
1	102.6	28.9	2.59	0	0	0
5	171.9	85.3	31.3	3.6	0.3	0
10	194.1	106.3	48.2	10.9	2.2	0
30	218.8	130.3	70.1	26.2	10.7	1.66
90	233.6	145.0	84.3	38.8	21.0	7.2
180	239.6	151.0	90.3	44.4	26.2	11.2
210	308.7	221.0	160.4	72.5	39.0	14.1
270	326.2	238.3	177.3	87.6	51.6	21.5
360	334.6	246.6	185.5	95.5	59.0	27.4
730	344.8	256.8	195.7	105.5	68.6	36.2

(a)

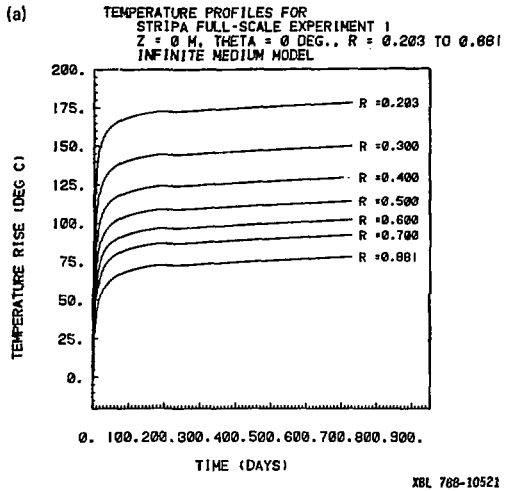

(b)

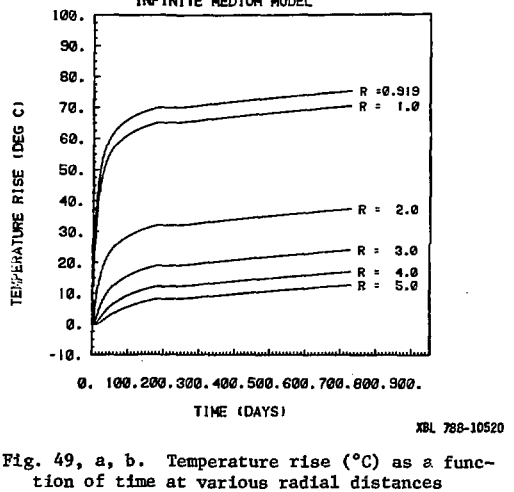

Fig. 49, a, b. Temperature rise (°C) as a function of time at various radial distances along heater mid-plane, Stripa full-scale Experiment 1 (3.6 kW), Model Series 2, infinite medium model. Thermal conductivity = 3.2 W/m°C, thermal diffusivity = 1.47×10^{-6} m^2/s.

(a)

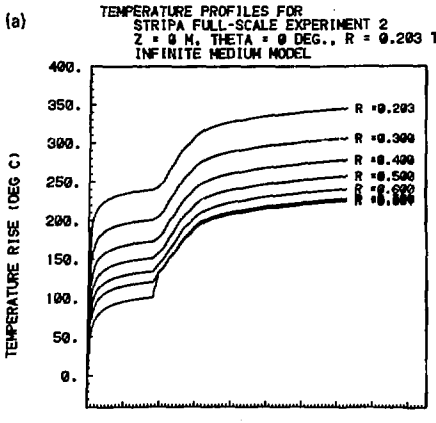

(b)

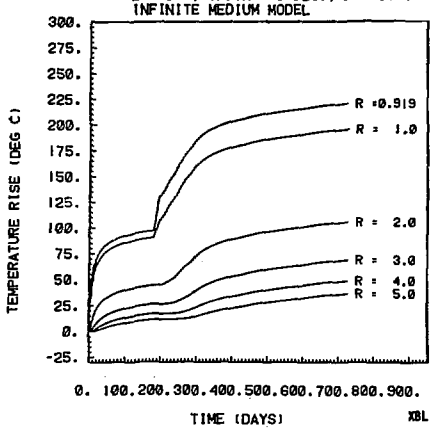

Fig. 50, a, b. Temperature rise (°C) as a function of time at various distances from axis of central heater along a radius passing through one peripheral heater, Stripa full-scale Experiment 2 (5 kW with eight 0.72 kW peripheral heaters), Model Series 2, infinite medium model. Thermal conductivity = 3.2 W/m°C, thermal diffusivity = 1.47×10^{-6} m^2/s.

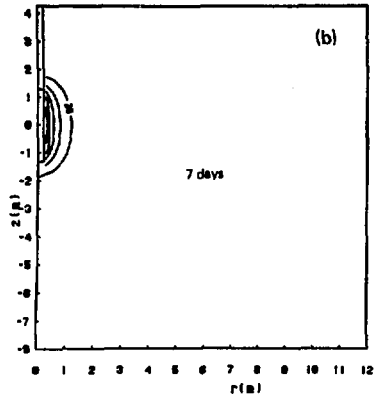

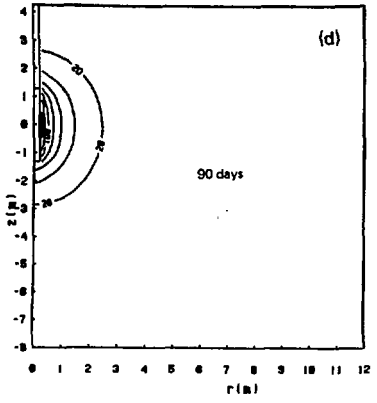

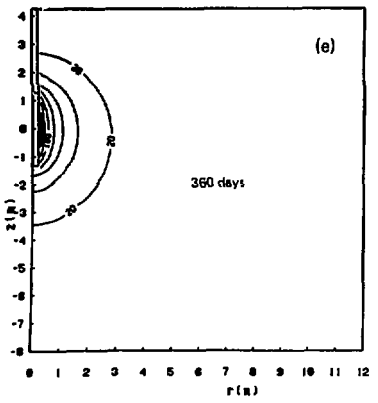

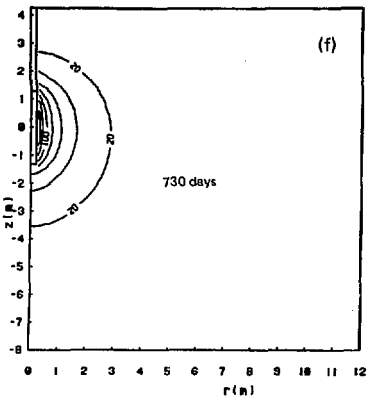

Fig. 52b, d, e, f. Isotherms of temperature rise (°C) in Stripa full-scale Experiment 1 (3.6 kW) at time = 7, 90, 360 and 730 days; vertical section, Model Series 2, isothermal boundary model. Thermal conductivity = 3.2 W/m°C, thermal diffusivity = 1.47×10^{-6} m^2/s.

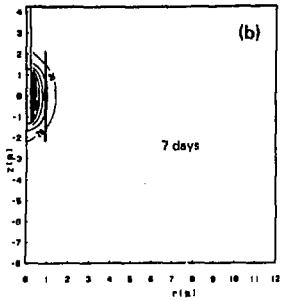

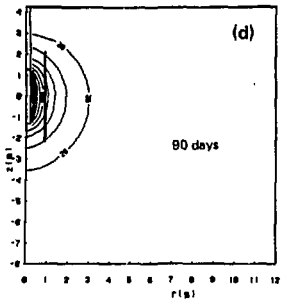

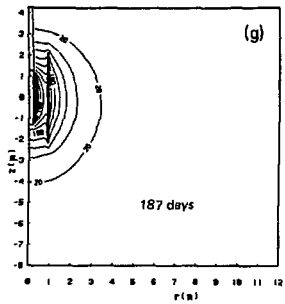

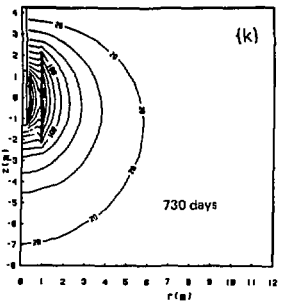

Fig. 54b, d, g, k. Isotherms of temperature rise (°C) in Stripa full-scale Experiment 2 (5 kW with eight 0.72 kW peripheral heaters) at time = 7, 90, 187, and 730 days; vertical section through axes of central heater and one peripheral heater, Model Series 2, isothermal boundary model. Thermal conductivity = 3.2 W/m°C, thermal diffusivity = 1.47×10^{-6} m^2/s.

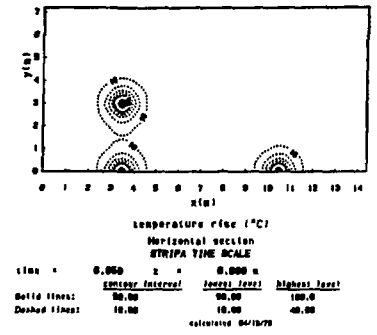

(b) 7 days

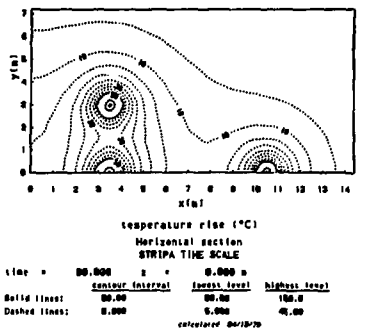

(d) 90 days

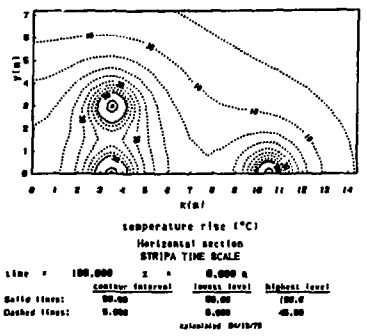

(e) 180 days

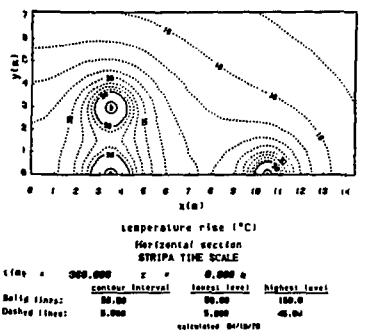

(f) 360 days

Fig. 55b, d, e, f. Isotherms of temperature rise (°C) in Stripa time-scaled experiment (constant power 1.125 kW) at time ≈ 7, 90, 180, 360 days; horizontal section through mid-plane of the heaters, *Model Series 2.* Thermal conductivity = 3.2 W/m°C, thermal diffusivity = 1.47×10^{-6} m^2/s.

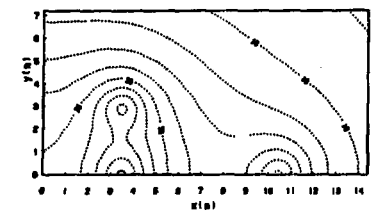

(a) z = 1 m

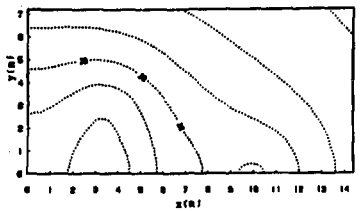

(b) z = 2 m

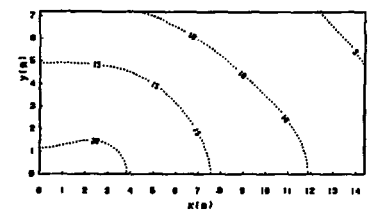

(d) z = 4 m

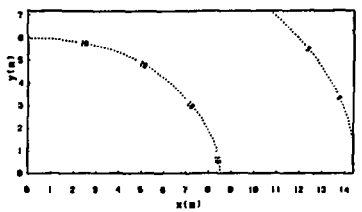

(e) z = 6 m

Fig. 56a, b, d, e. Isotherms of temperature rise (°C) in Stripa time-scaled experiment (constant power 1.125 kW) at the end of 73 days; horizontal section at vertical distances of 1, 2, 4, 6 m from mid-plane, Model Series 2. Thermal conductivity = 3.2 W/m°C, thermal diffusivity = 1.47×10^{-6} m^2/s.

- As Stripa granite has higher thermal diffusivity than average granite, a quasi-steady state is reached more promptly than in Model Series 1 (cf. Tables 3 and 5).
- A delay of 180 days for the turn-on of the peripheral heater is sufficient (Fig. 50a).
- The ring of peripheral heaters raises the temperature of the rock within its perimeter by about 100°C a few months after turn on but does not introduce additional thermal gradients. This is clear from the nearly parallel curves in Fig. 50a.
- Midway between the two full-scale experiments (r = 11 m), the rock temperature is raised by 4°C by Experiment 1 and 11°C by Experiment 2. Thermal interference between the two experiments is, therefore, minor.
- Maximum heat flux into the heater drift was found to be slightly less than one-third of the total power of the heater array in Experiment 2 with isothermal boundary conditions.
- Time-scaled heaters at 3 m spacing interact at the 30°C level in 90 days while those at 7 m spacing only interact at the 20°C level even after 730 days when the 40°C isotherms have already merged for the more closely spaced heaters (Fig. 55). Thus the time-scaled experiment will demonstrate the effect of different canister spacing in a repository over a period of 20.4 years.
- Various horizontal sections (Fig. 56) illustrate that at short vertical distances from the time-scaled heater array, the presence of the individual heaters can still be recognized. However, further above (e.g. 6 m above mid-plane), no trace of individual heaters can be distinguished. Thus the 10°C incremental isotherm is an ellipsoidal surface after the heaters have been operating for two years.
- Throughout the duration of the experiments the temperature rise is less than 100°C at a radius of 2 m from the central heater in Experiment 2 (Fig. 53, 54) and less than 50°C, 1 m from any heater in Experiment 3 (Fig. 55), so the high temperature zones are localized in all three experiments. Therefore, in order to physically simulate the thermal effects on the excavation and repository scales, it is necessary to carry out other types of heating experiments whereby a large volume of

rock is heated up, e.g., by using many electrical heaters, by dielectric heating or by pressurized hot water heating.

8. SUMMARY AND CONCLUSION

Thermal conduction calculations have been carried out for the three heater experiments at Stripa using a semi-analytic method based on the Green's function solution of a finite length line source in a semi-infinite medium as well as a numerical model based on the integrated-finite-difference technique. The more important results can be summarized as follows:

- o Geometric attenuation is an important factor. Therefore, in evaluating the near-field thermal effects of a planar repository, the detailed geometrical arrangement of the waste canisters should be taken into account.
- o Results from a semi-analytic constant power finite line source model are in close agreement with those from a constant flux numerical model.
- o The boundary condition at the floor of the heater drift has negligible effect on the temperature field close to the mid-plane of the full scale heaters in the first few months of operation.
- o The correct boundary condition should lie somewhere between the infinite medium and isothermal boundary idealizations.
- o The temperature fields within a 1 m radius of the central heater in the two full-scale experiments approach a quasi-steady state 3 or 4 months after the turn-on of the central heater or the peripheral heaters.
- o The local temperature gradient within a 0.5 m radius of the central heater reaches a maximum within a few days of start-up and hardly changes thereafter.
- o Thermal gradients near the outer edge of the heated zone decline with time.
- o There is a vertical temperature gradient throughout the duration of the experiments.
- o A ring (0.9 m radius) of eight 0.72 kW peripheral heaters will provide a nominally uniform temperature rise within its perimeter a few weeks after turn-on, thereby increasing the ambient rock

temperature just as it would in a repository when a large array of waste canisters interact. The maximum temperature rise due to the peripheral heaters is approximately 100°C.

- The scaling for the time-scaled experiment is correct in the sense that the temperature increases 0.5 m from a 1.125 kW time-scaled heater 30 days after turn-on is equal to that 1.6 m from a 3.6 kW full-scale heater 306 days after turn-on.
- Two time-scaled heaters at 3 m (corresponding to 9.6 m in full scale) spacing interact at the 30°C level in 90 days (corresponding to 918 days in full scale) and at the 40°C level in 730 days (corresponding to 20.4 years in full scale), whereas two time-scaled heaters at 7 m (corresponding to 22.4 m in full scale) interact only at the 20°C level in 730 days.
- Toward the end of the time-scaled experiment the 5°C and 10°C incremental isotherms have ellipsoidal shapes, as expected for a planar repository.
- Maximum temperature rise in the rock has been predicted to be 178°C for the 3.6 kW full-scale heater experiment, 345°C for the full-scale experiment with a 5 kW central heater and eight 0.72 peripheral heaters, and less than 200°C for the time-scaled experiment.
- The high temperature zone is localized throughout the duration of all three experiments. In the second full-scale experiment (5 kW) the 100°C incremental isotherm lies within a 2 m radius while in the time-scaled experiment the 50°C incremental isotherm has a radius less than 1 m.
- It can be concluded that while the type of heater experiments modeled in the present work provides indispensable information on the thermal effects in the immediate vicinity of an individual canister as well as the effect of different spacing on thermal interaction between adjacent canisters, it will be necessary to carry out larger scale heating experiments to evaluate the thermal effects on the excavation and repository scales.

ACKNOWLEDGMENTS

We would like to acknowledge the assistance of J. Chin, N. Littlestone, and J.S. Remer for their assistance in computer programming. We also wish to extend our thanks to Drs. C.W. Miller and P. Nelson for a number of comments which helped to improve the clarity of the presentation. We also thank C. Goranson and M. Lippmann for their help in the use of the CCC model.

REFERENCES

Bäckblom, G., Appendix I in Carlsson, H., A Pilot Heater Test in the Stripa Granite, Lawrence Berkeley Laboratory Report LBL-7086, SAC-06 (1978).

Carlsson, H., A Pilot Heater Test in the Stripa Granite, LBL-7086, SAC-06 (1978).

Carslaw, H.S. and Jaeger, J.C., Conduction of Heat in Solids (Oxford University Press, 1959).

Chan, T. and Ballentine, L.E., Physics and Chemistry of Liquids 2, 165 (1971).

Chan, T. and Remer, J.S., Thermal and Thermomechanical Modeling of in situ Heater Experiments at Hanford: Preliminary Results, Lawrence Berkeley Laboratory Report LBL-7069 (1978).

Cruse, T.A. and Rizzo, F.J. (eds.), "Boundary-Integral Equation Method: Computational Applications in Applied Mechanics," Proc. Am. Soc. Mech. Eng. Spec. Pub. 11 (1975).

Edwards, A.L., TRUMP: A Computer Program for Transient and Steady State Temperature Distribution in Multidimensional Systems, Lawrence Livermore Lab. Rpt. UCRL-14754, Rev. 3., 1972.

Hodgkinson, D.O., Deep Rock Disposal of High Level Radioactive Waste: Transient Heat Conduction from Dispersed Blocks, AERE-R-8763 (1977).

Jackson, J.D., Classical Electrodynamics, 2nd edition (Wiley, New York, 1975).

Lippmann, J.M., Tsang, C.F. and Witherspoon, P.A., Paper SPE 6537, presented at 47th Annual California Regional Meeting of the Soc. of Petrol. Eng. of AIME, Bakersfield, California, April 1977.

McElroy, M.B., "Data Acquisition, Handling and Display for the Heater Experiments at Stripa," LBL-7062, 1978.

Morse, P.M. and Feshbach, H. Methods of Theoretical Physics (McGraw-Hill, New York, 1953).

Narasimhan, T.N. and Witherspoon, P.A., Water Resour. Res., 12, No. 1., p. 57-64, 1976.

Mufti, I.R., Journ. Geophys. Res. 76, 8568 (1971).

Pratt, H.R., Schrauf, T.A., Bills, L.A., and Hustrulid, W.A., Thermal and Mechanical Properties of Granite: Stripa, Sweden, Summary Report TR-77-92 (Terratek, Salt Lake City, Utah, 1977).

Witherspoon, P.A. and Degerman, O., Swedish-American Cooperative Program on Radioactive Waste Storage in Mined Caverns Program Summary, LBL-7049, SAC-01 (1978).